Neurochemistry

JOURNAL OF NEUROCHEMISTRY | 2008 | 106 | 613–624 doi: 10.1111/j.1471-4159.2008.05414.x

Spastin oligomerizes into a hexamer and the mutant spastin (E442Q) redistribute the wild-type spastin into filamentous microtubule

D. V. Krishna Pantakani,* Lakshmipuram S. Swapna,† Narayanaswamy Srinivasan† and Ashraf U. Mannan*

**Institute of Human Genetics, University of Goettingen, Goettingen, Germany*

†*Molecular Biophysics Unit, Indian Institute of Science, Bangalore, India*

Abstract

Spastin, a member of the ATPases associated with various cellular activities (AAA) family of proteins, is the most frequently mutated in hereditary spastic paraplegia. The defining feature of the AAA proteins is a structurally conserved AAA domain which assembles into an oligomer. By chemical cross-linking and gel filtration chromatography, we show that spastin oligomerizes into a hexamer. Furthermore, to gain a comprehensive overview of the oligomeric structure of spastin, we generated a structural model of the AAA domain of spastin using template structure of VPS4B and p97/VCP. The generated model of spastin provided us with a framework to classify the identified missense mutations in the AAA domain from hereditary spastic paraplegia patients into different structural/functional groups. Finally, through co-localization studies in mammalian cells, we show that E442Q mutant spastin acts in a dominant negative fashion and causes redistribution of both wild-type spastin monomer and spastin interacting protein, RTN1 into filamentous microtubule bundles.

Keywords: hereditary spastic paraplegia, hexamer, oligomerization, spastin.

J. Neurochem. (2008) **106**, 613–624.

Mutation in the *SPAST* (*SPG4*) gene is the single most common cause for hereditary spastic paraplegia (HSP) and accounts for ~40% of autosomal dominant cases of HSP (Hazan *et al.* 1999; Fonknechten *et al.* 2000; Lindsey *et al.* 2000). The *SPG4* subtype is considered as pure form of HSP and clinically characterized by lower limb spasticity, weakness, hyperreflexia, and often mild vibratory sense impairment in the toes (Harding 1983; Fink 2003). The *SPAST* gene encodes for spastin protein, which belongs to the ATPases associated with various cellular activities (AAA) family of proteins (Patel and Latterich 1998; Hanson and Whiteheart 2005). These ATPases are principally characterized by the AAA domain, often located in the C-terminal part of the protein, whereas the N-terminal part contains recognition sites for substrates and adaptors (Patel and Latterich 1998; Hanson and Whiteheart 2005). All types of mutations are reported in the *SPAST* gene, including missense, nonsense, splice site mutations, and small insertions/deletions suggesting haploinsufficiency as the pathogenic mechanism (Fonknechten *et al.* 2000; Lindsey *et al.* 2000). Interestingly, almost all the missense mutations are located in the C-terminal AAA domain (Fonknechten *et al.* 2000; Lindsey *et al.* 2000) and recent studies suggests that these mutations might exert a dominant negative effect on the molecular function of spastin (Errico *et al.* 2002; Evans *et al.* 2005).

Numerous studies used different biological systems to determine the molecular function of spastin, in an attempt to elucidate its role in the pathogenesis of HSP. Majority of

Received August 16, 2007; revised manuscript received March 28, 2008; accepted April 2, 2008.

Address correspondence and reprint requests to Dr Ashraf U. Mannan, Institute of Human Genetics, University of Goettingen, Heinrich-Dueker-Weg 12, D-37073, Goettingen, Germany.
E-mail: amannan@gwdg.de

Abbreviations used: AAA, ATPases associated with various cellular activities; CSU, Contacts of Structural Units; DSP, dithiobis-succinimidyl propionate; GST, glutathione-S-transferase; HSP, hereditary spastic paraplegia; MIT, microtubule interacting and trafficking; MT, microtubule; PBS, phosphate-buffered saline; RTN, reticulon; SDS–PAGE, sodium dodecyl sulfate–polyacrylamide gel electrophoresis; VPS, vacuolar protein sorting.

these studies suggest that spastin plays a role in microtubule (MT) network dynamics (Errico *et al.* 2002; McDermott *et al.* 2003; Evans *et al.* 2005; Roll-Mecak and Vale 2005; Salinas *et al.* 2005). Expression of spastin in cultured cells revealed dynamic interaction between spastin and the MT and also partial loss of MT network can be detected in the cells over-expressing spastin (Errico *et al.* 2002; McDermott *et al.* 2003; Evans *et al.* 2005). Lately, it has been shown that spastin possesses direct MT-severing activity (Evans *et al.* 2005; Roll-Mecak and Vale 2005) and it can also bundle MTs (Salinas *et al.* 2005). The role of spastin in MT-mediated axonal transport is further supported by *in vivo* studies in *Drosophila*, zebra fish, and mouse, where knockdown of spastin results in abnormal MT dynamics in the neurons (Sherwood *et al.* 2004; Trotta *et al.* 2004; Tarrade *et al.* 2006; Wood *et al.* 2006). However, the role of spastin in membrane trafficking and vesicular transport is now emerging. Recently, several studies, including from our group, showed that spastin interacts with different components of vesicular transport process such as chromatin modifying protein 1B (Reid *et al.* 2005), Zinc finger, FYVE domain containing 27 (Mannan *et al.* 2006b), atlastin (Evans *et al.* 2006; Sanderson *et al.* 2006), and reticulon1 (RTN1) (Mannan *et al.* 2006a). Spastin mediates its interaction with vesicular proteins through its N-terminal region, which contain the MT interacting and trafficking (MIT) domain. The MIT domain is common to a group of proteins involved in endocytosis and intracellular trafficking, such as suppressor of K(+) transport growth defect 1 and sortin nexin 15 (Ciccarelli *et al.* 2003). It is also present in spartin, mutations in which cause a complicated autosomal recessive form of HSP, namely, Troyer syndrome (Patel *et al.* 2002). The fact that spastin contains MIT domain and localizes in punctate vesicular structures in cultured cells; further strengthen its role as mediator of vesicular transport processes.

Despite recent advancement in molecular studies, a comprehensive function of spastin has not yet been elucidated. It appears that spastin is a multifaceted protein with versatile role in cellular events. The functional diversity of spastin can be attributed to different functional regions of spastin such as the nuclear export sequence, nuclear localization sequence, transmembrane motif, MIT, and more importantly the AAA domain as almost all missense mutations reported in spastin are in the AAA domain. The central feature of AAA family is a structurally conserved AAA domain which binds to ATP and assembles into an oligomer. The AAA domain contains Walker A and B motifs and also several other motifs that distinguish it from classic P loop NTPases (Confalonieri and Duguet 1995; Frickey and Lupas 2004). Apart from the AAA domain, these proteins consist of various other domains, which interact with adaptor proteins to generate the structural and functional diversity of the family (Confalonieri and Duguet 1995; Frickey and Lupas 2004; Hanson and Whiteheart 2005). Majority of the AAA proteins function as molecular machines which disassemble protein complexes. They couple energy derived from ATP hydrolysis to achieve their role by promoting conformational changes or remodeling in target proteins (Patel and Latterich 1998; Hanson and Whiteheart 2005). The phylogenetic analysis based on sequence similarity places spastin into a subfamily called meiotic group of AAA proteins (Frickey and Lupas 2004). The notable members of this group are katanin (p60) (McNally and Vale 1993) and vacuolar protein sorting 4 (suppressor of K(+) transport growth defect 1) (Yoshimori *et al.* 2000). Katanin is a MT-severing protein and forms an oligomer in the ATP-bound state (Hartman and Vale 1999). VPS4, which also harbors a MIT domain in its N-terminal region, is involved in vacuolar sorting and endosomal transport. The wild-type VPS4 protein cycles between soluble, inactive low molecular weight complexes and active, membrane-associated double-ring structures (10–12 subunits) (Babst *et al.* 1998; Scott *et al.* 2005). Based upon sequence similarity it can be postulated that spastin might also form an oligomeric structure to render its function. A very recent study reported that the AAA domain of spastin can assemble into hexamer (White *et al.* 2007). In their study, the hexameric state of AAA domain of spastin was very unstable as it could not be stabilized even in the presence of slowly hydrolysable ATPγS and they could only trap the hexamer, when they used the Walker B E442Q mutant form of spastin AAA domain.

In the present study, we used full-length spastin and showed through chemical cross-linking and gel filtration chromatography that wild-type spastin oligomerizes into a hexamer. Our results suggest that N-terminal region of spastin might play a critical role in the formation of a stable hexamer. Furthermore, a computational model of the oligomeric form of spastin was generated, which was used to elucidate the structural basis of the stability of the hexameric structure of spastin.

Materials and methods

Generation of GST–spastin construct, expression, and purification

The human short isoform of spastin initiating from the alternative start codon (M87) was amplified by RT-PCR using a primer pair, M87f, GAATTCATGGCAGCCAAGAGGAGCTCCGGGG and M87r, AAGCTTGTTAAACAGTGGTATCTCCAAAGTCCTTG with Takara Taq polymerase (Takara Bio Inc., Japan) from human brain cDNA (BD Biosciences, Palo Alto, CA, USA). The amplified RT-PCR product was cloned into *Eco*RI and *Hind*III sites of pET41a vector (Qiagen, Hilden, Germany). Any possible incorporation of mutation during PCR amplification was excluded by complete sequencing of the construct. The spastin-pET41a construct was transformed into BL21-DE3 strain of *Escherichia coli* and bacterial culture was grown at 30°C until 0.8 optical

density at 620 nm was reached then induced with 0.5 mM isopropyl β-D-1 thiogalactopyranoside for 4 h. The induced bacteria were lysed by sonication either in buffer A (with 2 mM ATP) or B (with 5 mM $MgCl_2$) containing 50 mM Tris–HCl, pH 8.0, 200 mM NaCl, 10% glycerol, 5 mM dithiothreitol, and protease inhibitors. Bacterial debris from protein extract was cleared by centrifugation at 14 000 *g* for 30 min at 4°C. The cleared protein extract was passed through glutathione–agarose column (Sigma, St Louis, MO, USA) pre-equilibrated with buffer A/B and washed with 10 column volumes of buffer A/B. The bound protein was eluted using 10 mM reduced glutathione in either buffer A or B. The glutathione-S-transferase moiety was cleaved from the purified GST-spastin protein by overnight incubation with thrombin enzyme (Sigma) at 4°C. The cleaved GST was removed from spastin by glutathione–agarose binding.

ATPase assay

The activity of the purified spastin protein was assayed by using 250 ng of purified protein in a 200 μL reaction buffer containing 50 mM Tris–HCl, pH 7.5, 5 mM $MgCl_2$, and varying amounts of ATP (Sigma). The reaction was then incubated at 37°C for 30 min and was stopped by adding 50 μL of malachite green reagent (BioAssay Systems, Hayward, CA, USA) and measured the optical density at 620 nm on a 96-well plate reader and calculated the amount of inorganic phosphate released by ATPase activity of the spastin from the standard curve. The absorbance of control samples containing the same amount of ATP without the enzyme was subtracted from the overall value of the samples. The K_m and V_{max} of spastin ATPase was calculated using non-linear regression analysis (GraphPad Prism 4.0; GraphPad Software Inc., San Diego, CA, USA).

Chemical cross-linking using dithiobis-succinimidyl propionate

Chemical cross-linking was performed using homobifunctional, thiol-cleavable dithiobis-succinimidyl propionate (DSP; Pierce Biotechnology, Rockford, IL, USA) with final concentrations ranging from 0.2 to 1 mM in reaction buffer (100 mM Phospaste, pH 7.2, and 150 mM NaCl) using 5 μg of purified spastin protein in total volume of 30 μL. Reaction mixtures were then incubated at ~25°C for 20 min and stopped by adding 1 M Tris–HCl, pH 8.0, and non-reducing Laemmli loading dye. The samples were then electrophoresed without boiling on 4–12% Bis–Tris gradient gel (Invitrogen, Paisley, UK) and transferred onto nitrocellulose membrane (Hybond C-extra; Amersham Bioscience, Bucks, UK) and probed with rabbit polyclonal anti-spastin antibody, 54S1 (kind gift from Professor Elena I. Rugarli).

Gel filtration chromatography and immunoblotting

For gel filtration chromatography, we used Superdex 200 PC 3.2/30 HPLC column system (Amersham Biosciences); the column bed volume was 2.4 mL. The purified GST-spastin or cleaved spastin (either with ATP or without ATP) was centrifuged at 15 700 *g* for 10 min and about 50 μg of protein (1 μg/μL) was loaded onto the Superdex 200 column, which was pre-equilibrated with either buffer A or B. The protein elution was performed at a flow rate of 40 μL/min and about 60 fractions (40 μL each) were collected. The molecular weight of native spastin and GST-spastin oligomer was extrapolated from standard curve plotted with the values obtained from the protein molecular weight of standard markers (Amersham Bioscience). The protein fractions were resolved on 10% sodium dodecyl sulfate–polyacrylamide gel electrophoresis (SDS–PAGE) and transferred onto nitrocellulose membrane (Amersham Bioscience). Western blot was performed with polyclonal anti-spastin antibody, 54S1 as described previously (Errico *et al.* 2004).

Modeling of tertiary and quaternary structure of the AAA domain of spastin

The complete AAA domain sequence of spastin was searched against PDB (Berman *et al.* 2000) using the BLAST program (Alstchul Lab, NCBI, Bethesda, MD, USA, http:www.ncbi.nlm.nih.gov/blast) (Altschul *et al.* 1997), with default parameters, to identify closely related homologs of spastin with known 3-D structure. The AAA ATPase domain of spastin was modeled on the basis of the tertiary structures of two templates (PDB codes: 1xwi and 1s3s) (Dreveny *et al.* 2004; Scott *et al.* 2005) using MODELLER version 8.0 (Sali Lab, UCSF, San Francisco, CA, USA, http://www.salilab.org/modeller) (Sali 1995). The generated models were energy minimized using the Kollman united atom force field in SYBYL (Tripos Inc., St. Louis, MO, USA) to ensure acceptable geometry and to relieve short contacts. The overall fit of the sequence to the template was checked using Verify 3D (Luthy Lab, University of California, CA, USA; http://www.nihserver.mbi.ucla.edu/Verify_3D) (Luthy *et al.* 1992). The copies of modeled tertiary structure were assembled to form a hexameric quaternary assembly on the basis of the hexameric template (1s3s). This modeled quaternary structure was energy minimized using SYBYL. The interfacial residues between the monomers were extracted using the Contacts of Structural Units (CSU) program (Sobolev Lab, Weizman Institute of Sciences, Israel, http://www.bip.weizmann.ac.il/oca-bin/lpccsu) (Sobolev *et al.* 1999) and the crucial residues were short listed by manual inspection and used for further analysis.

Generation of constructs, immunoprecipitation, and immunocytochemical analysis

The generation of spastin-pCS2, spastin-pEGFP, and RTN1-pQM constructs were described previously (Mannan *et al.* 2006a). To introduce the E442Q and R499C missense mutations in spastin, we used spastin-pEGFP plasmid DNA as template and the mutation was introduced by using the QuikChange site-directed mutagenesis kit (Stratagene, La Jolla, CA, USA). The presence of the point mutation was confirmed by DNA sequencing. The primers used to generate the point mutations were: E442Qf, CCTTCTATAATTTTATAGATCAAGTTGATAGCCTTTTGTGTG; E442Qr, CACACAAAAGGCTATCAACTTGATCTATAAAAATTATAGAAGG; R499Cf, GATGAGGCTGTTCTCAGGTGTTTCATCAAACGGGTATATG; R499Cr, CATATACCCGTTTGATGAAACACCTGAGAACAGCCTCATC. Immunoprecipitation assay was performed as described previously (Mannan *et al.* 2006a). For immunocytochemistry analysis, the NIH3T3 cells were seeded into two chamber culture slides (BD Falcon, Palo Alto, CA, USA) for transfection. After 24 h, cells were co-transfected with the c-Myc-spastin and Gfp-E442Q-spastin/Gfp-R499C-spastin constructs using Lipofectamine 2000 reagent (Invitrogen). Following 24–30 h of transfection, the cells were

washed two times with phosphate-buffered saline (PBS) and fixed in 4% *p*-formaldehyde in PBS for 30 min. The transfected cells were permeabilized and blocked by incubating in blocking solution [30% goat serum (Invitrogen), 20 mM phosphate buffer, pH 7.2, 450 mM NaCl, and 0.3% Triton X-100] for 30 min. In the next step, the cells were incubated with a c-Myc antibody (Dunn Labortechnik, Asbach, Germany) in a dilution of 1 : 200 for 2 h at ~25°C. Thereafter, cells were washed three times for 10 min each with PBS and then incubated with anti-rabbit IgG conjugated with Cy3 (Sigma) at a dilution of 1 : 100 for 1 h at ~25°C. Finally, the stained cells were washed again three times for 10 min each with PBS and let to air dry. The culture flask was detached from the glass slide according to the manufacture's instruction and VectaShield solution (Vector Laboratories, Burlingame, CA, USA) was applied before mounting with a coverslip. Slides were observed using a confocal microscope (Olympus, Hamburg, Germany) and images were processed by the Cell-f program (Soft Imaging System, Muenster, Germany).

Results

Expression and purification of short isoform of spastin

Spastin has many isoforms, the long isoform and a more abundant nuclear/cytoplasmic short isoform encoded by an alternative start site, corresponding to residue 87 of full-length spastin (long isoform) (Claudiani *et al.* 2005). The short isoform is likely to be the most soluble form in the cytoplasm as it lacks the putative transmembrane motif; therefore, a high level of expression of this isoform can be achieved in bacteria. For these reasons, we chose short isoform of spastin (referred as spastin) for our studies and cloned it into bacterial expression vector. Analysis of recombinant spastin protein, which was affinity purified from bacterial protein extract and resolved by SDS–PAGE revealed a high level of expression in soluble fraction

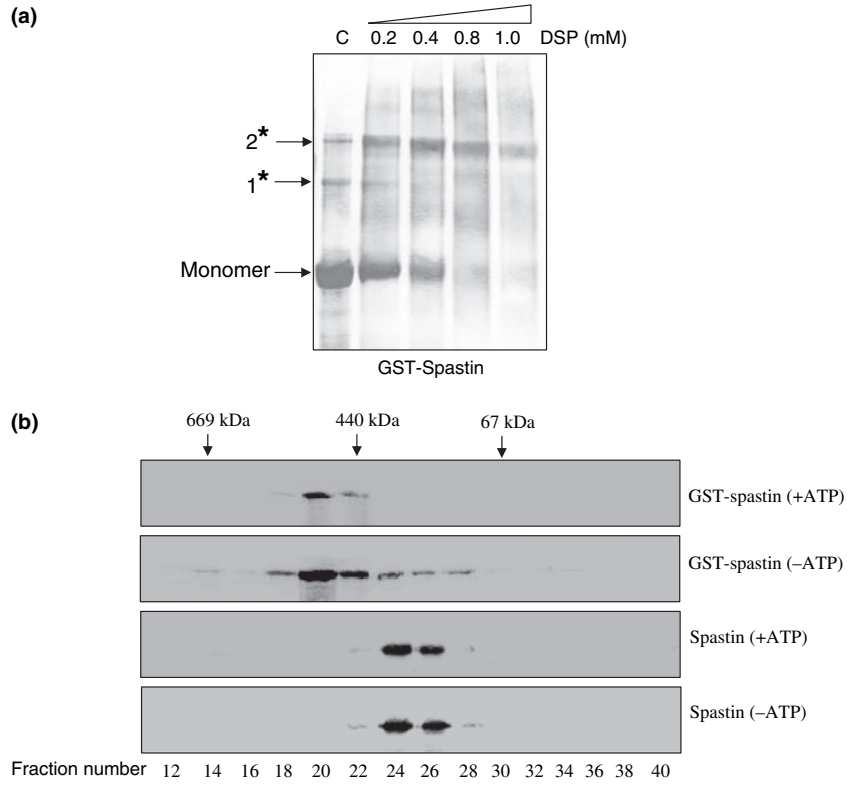

Fig. 1 Oligomerization of spastin. Chemical cross-linking of spastin by dithiobis-succinimidyl propionate (DSP). Purified GST-spastin was subjected to chemical cross-linking with DSP and was resolved in SDS–PAGE under non-reducing condition and transferred to nitrocellulose membrane, western blot was performed with spastin polyclonal antibody. Asterisks denote higher order cross-linked oligomeric spastin. Two major forms of oligomeric spastin were detected after cross-linking, probably an intermediate form designated as asterisk 1 and predominant hexameric form represented as asterisk 2. The formation of hexameric spastin was dependent upon the concentration of DSP, at high concentration of DSP (1 mM) only hexameric form of spastin exists. Interestingly, even in the absence of DSP cross-linking (denoted as lane C), besides predominant monomeric spastin, a fraction of both higher order oligomeric spastin were detectable (a). HPLC gel filtration chromatography. The purified GST-spastin or cleaved spastin (either with ATP or without ATP) was subjected to gel filtration chromatography on Superdex 200 HPLC column. The aliquot of eluted fractions were immunoblotted with anti-spastin antibody. The elution peaks for marker proteins (in kDa) are indicated across the top of the immunoblot. The number of the eluted fraction in the chromatography is represented below the immunoblot (b).

(Supplementary Fig. S1a) and the purified recombinant spastin protein was enzymatically active as confirmed by ATPase assay, with a K_m value of 1.497 ± 0.24 and V_{max} of 0.2874 ± 0.023 (Supplementary Fig. S1b).

Wild-type spastin forms a hexamer

Majority of the AAA proteins function as oligomer. To determine whether spastin can also assemble as an oligomer, we first cross-linked purified GST-spastin with thiol-cleavable chemical cross-linker DSP. Resolving of cross-linked GST-spastin by SDS–PAGE suggested that spastin is able to form an oligomeric structure (Fig. 1a). We observed an intermediate oligomeric form as well as a hexameric form of spastin in our cross-linking studies, which was dependent on the concentration of DSP (Fig. 1a). At higher concentration of DSP, hexamer was the most prominent form of spastin (Fig. 1a).

To find out the precise oligomeric state of spastin, we next analyzed GST-spastin by gel filtration chromatography. As most AAA proteins are known to assemble into oligomers in an ATP-dependent manner, but remain monomeric in the absence of nucleotide, the first set of gel filtration assay was performed in presence of ATP. The GST-spastin purified in presence of ATP was subjected to gel filtration chromatography and the eluted fractions were analyzed by western blot using spastin antibody. Based upon our gel filtration analysis, it appears that the GST-spastin forms a hexamer as it eluted at a native size of ~530 kDa (monomer is ~88 kDa), which is consistent with the proposed hexameric state of GST-spastin (Fig. 1b). To investigate whether the oligomeric state of spastin is ATP dependent or independent, we performed gel filtration assay in an ATP depleted condition. Analysis of elution profile revealed GST-spastin in absence of ATP also eluted at a native size of ~530 kDa; however, spastin eluted in multiple fractions, showing a diffuse pattern of elution (Fig. 1b). To exclude any possibility of artifact generated due to GST moiety, we cleaved the GST tag from recombinant spastin and performed gel filtration assay with GST-free spastin protein in the presence and absence of ATP. The elution pattern of the gel filtration assay revealed that spastin forms a hexameric structure, which was eluted at native size of ~350 kDa (Fig. 1b). ATPase assay was performed with all the eluted fractions and fractions containing spastin oliogmers were enzymatically active (data not shown).

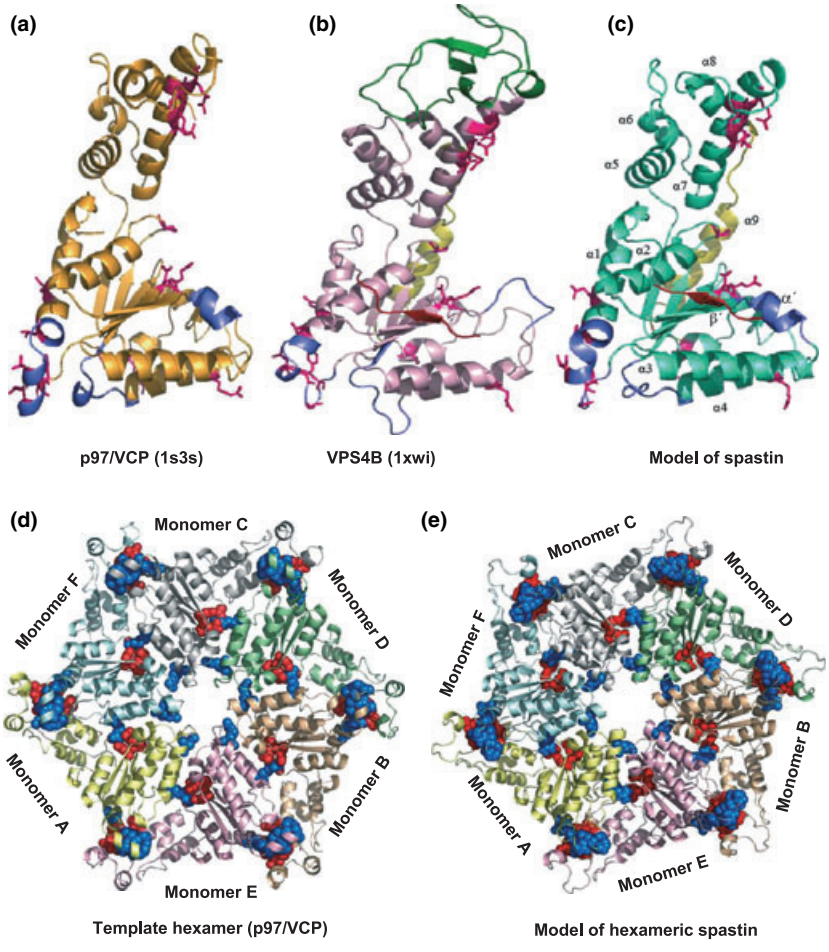

Fig. 2 Structural models of spastin AAA domain. The tertiary structures of p97/VCP (a), VPS4B (b), and modeled AAA ATPase domain of spastin (c) are shown as ribbon diagrams. Regions undergoing conformational change are colored blue and interacting residues between the monomers are colored magenta in all the three structures. The beta domain of VPS4B is marked in green (b). The N-terminal beta strand (β′) unique to meiotic AAA ATPases is highlighted in brown (b and c). The C-terminal strand unique to meiotic AAA ATPases is painted olive green in (b and c). The structures of template hexameric ring (d) and hexameric model of spastin AAA domain (e) are shown as ribbon structure. Each monomer is labeled in different color. The key interacting residues of both surfaces are depicted as spheres, in red and blue colors, respectively.

Modeled tertiary and quaternary structure of the AAA ATPase domain of spastin

Overview of modeled tertiary structure

A typical AAA ATPase domain consists of two subdomains, an N-terminal α/β domain followed by a smaller four-helix bundle. Our model shows that this tertiary structure is conserved in spastin (Fig. 2c). The Walker A and B motifs (355-GKT-357 and 409-DE-410) and the arginine finger (466-RR-467) of the second region of homology are the key sequence motifs which characterize the nucleotide binding site of the AAA ATPase domain. All these sequence motifs are conserved in the primary structure of spastin (Supplementary Fig. S2).

Comparison of AAA ATPase domains of spastin, VPS4B, and p97/VCP

The VPS4B protein (PDB code: 1xwi) (Scott *et al.* 2005), crystallized as a monomer, is the closest homolog of spastin with a crystal structure available (Fig. 2b) and show 50% sequence identity over the length of the domain (Fig. S2). The sequence and structural similarity between the VPS4B and spastin domains is quite high in the regions of secondary structures, whereas the loops show some variations (Fig. 2b and c and Fig. S2). The main difference is the absence of beta domain at the C-terminus of VPS4B, which is a feature of all vacuolar sorting proteins (Fig. 2b). The closest homolog of known structure which forms a hexamer is D1 domain of p97/VCP (PDB code: 1s3s) (Dreveny *et al.* 2004) (Fig. 2d). The AAA ATPase domain of spastin shares 36% sequence identity over the entire length with murine p97/VCP (Fig. S2). The overall tertiary structure of modeled spastin and p97/VCP domains (Fig. 2a and c) is similar except for the presence of a N-terminal β sheet and C-terminal α helix, which are characteristic of meiotic AAA ATPases such as spastin and VPS4B (Fig. 2a–c). The amino acid sequence of C-terminal region (~10 residues) of spastin is quite divergent from the other AAA ATPase domains (Fig. 2c).

Overview of quaternary structure of the spastin AAA ATPase domain

The hexameric model of spastin, which was generated based on the tertiary structure of VPS4B (Scott *et al.* 2005) revealed major short contacts at the interface regions. Therefore, we used the tertiary structures of both p97/VCP (Dreveny *et al.* 2004) and VPS4B (Scott *et al.* 2005) as joint templates for generating the tertiary structure of AAA ATPase domain of spastin with inter-monomer regions extrapolated from the topologically equivalent regions of p97/VCP. Using such a tertiary structural model we were able to generate an acceptable hexameric structure using p97/VCP as the template (Fig. 2e). The key interacting residues between the monomers of the AAA ATPase subunits of p97/VCP, extracted by the program CSU, are also conserved in VPS4B and spastin. The interacting partner amino acids for the key interacting residues as determined by CSU for both template and model are also reasonably conserved, which are summarized in supplementary Tables S1 and S2.

Furthermore, we classified known sets of HSP missense mutations identified in the AAA domain from the Human Gene Mutation Database Professional release 7.1 (http://www.biobase.de/hgmd/pro/start.php) into different structural/functional groups based upon the spastin model structure. We placed these mutations into four categories namely, active site, pore loop structure, monomer interface residues, and other mutations (Fig. 3a–k and Table S3).

Interaction of spastin monomers in the mammalian cells

To investigate whether spastin also forms an oligomeric structure under physiological condition, we decided to study interaction between differentially tagged spastin proteins in NIH3T3 cells. For co-immunoprecipitation and co-localization experiments, we utilized previously generated mammalian expression constructs in which spastin was tagged with c-Myc and Gfp moiety (Mannan *et al.* 2006a). We used a long isoform of spastin lacking exon 4 in these constructs because it localizes to punctate vesicles, which are distributed around perinuclear region of the cell displaying physiological relevance (Mannan *et al.* 2006a). For co-immunoprecipitation assay, the NIH3T3 cells were co-transfected with c-Myc-spastin and Gfp-spastin constructs. The total protein extract from co-transfected cells were immunoprecipitated with c-Myc antibody and subsequent, western blot analysis with Gfp antibody revealed a band of the size ~91 kDa corresponding to Gfp-spastin (Fig. 4a). However, Gfp-spastin band was undetectable in immunoblot when c-Myc antibody was omitted from the immunoprecipitation reaction (Fig. 4a). Next, we attempted to determine the interaction between wild-type spastin and mutant spastin protein. For these studies, we generated E442Q and R499C mutation in the AAA domain of Gfp-spastin protein (referred further as E442Q-spastin and R499C-spastin). The E442 residue localizes to conserve Walker B motif of AAA domain and this mutation allow ATP binding but prevent its hydrolysis (Evans *et al.* 2005). The R499C is a disease causing mutation, it constitutes the arginine finger of AAA domain and this mutant protein is unable to bind ATP. Co-immunoprecipitation studies with differentially tagged mutant and wild-type spastin proteins confirmed that both the mutant spastin proteins (E442Q and R499C) were able to associate with wild-type spastin in cells (Fig. 4b-c).

E442Q mutant spastin redistributes wild-type spastin and RTN1

We next attempted to determine the physiological relevance of interaction between spastin monomers by co-localization studies in mammalian cells. The NIH3T3 cells co-expressing

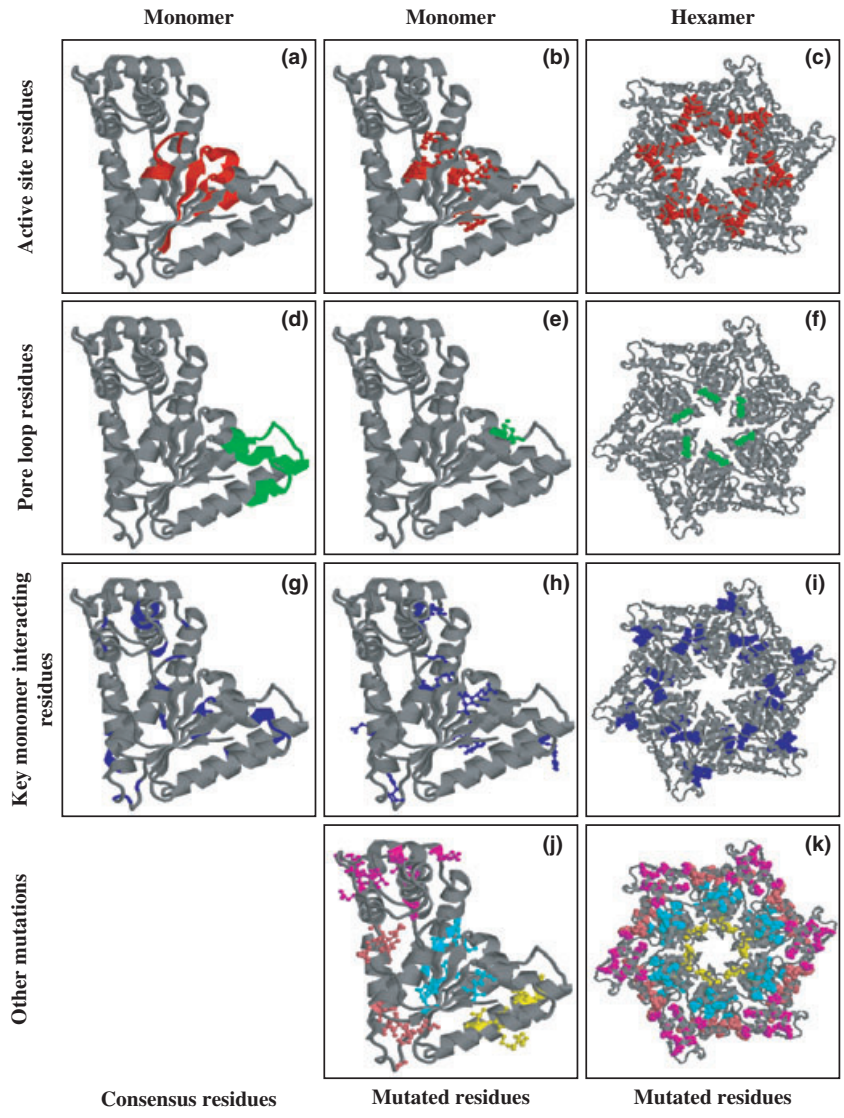

Fig. 3 Structural categorization of known HSP mutations. The HSP missense mutations identified in the AAA domain of spastin from database were categorized into four classes based upon the model of spastin. The first groups of mutations are in active site (a-c), the consensus amino acid residues are highlighted in red in the tertiary structure of spastin (a), the known HSP mutations from patients are shown as red ball and stick in tertiary and quaternary structure of spastin (b and c). The conserved pore loop residues are marked as green ribbon in spastin structure (d), the known HSP mutated residues categorized as pore loop mutations are depicted as green ball and stick in spastin monomer and hexamer (e and f). The key interacting residues between monomers required for oligomerization are shown in blue color in the tertiary structure of spastin (g), furthermore, the known set of HSP mutations in this group are also shown in the spastin monomer and hexamer (h and i). The HSP mutations, which could not be classified in above groups was designated as the other class of mutations. Labeling of these mutated residues in the modeled spastin structure revealed they can further be grouped in four clusters, which are labeled as magenta, orange, yellow, and light blue colors (j and k).

wild-type c-Myc-spastin and Gfp-spastin showed a strong co-localization in endosomal vesicles thus validating the interaction between the spastin monomers (Fig. 5a–d). After that we examined whether wild-type spastin also co-localizes with ATPase defective forms of spastin. The E442Q-spastin showed a filamentous expression pattern in the cytoplasm (Fig. 5e) and it was striking to observe that the expression of wild-type c-Myc-spastin was also filamentous in the same cell (Fig. 5f). The E442Q-spastin caused redistribution of wild-type spastin from punctate vesicles to abnormal filaments decorating MT (Fig. 5e–h). The R499C-spastin showed expression in punctate vesicles (Fig. 5i) and co-expression with wild-type c-Myc-spastin demonstrated strong co-localization in endosomal vesicles (Fig. 5i–l). Next, we evaluated possible effect of E442Q-spastin on intracellular distribution of RTN1, a spastin interacting protein (Mannan *et al.* 2006a). RTN1 is expressed in vesicles arising from endoplasmic reticulum and endosome. Co-expression of E442Q-spastin and E2-RTN1 in NIH3T3 cells resulted in redeployment of E2-RTN1 to filamentous MTs in the cytoplasm, where it shows co-localization with mutant spastin (Fig. 5m–p).

Discussion

In the present study, we determined the oligomeric state of spastin by cross-linking and gel filtration chromatography. Spastin forms intermediate state oligomeric structures, which is independent of nucleotide binding; however binding to ATP stabilizes the hexamer form of spastin. Next, we modeled tertiary and quaternary structure of the AAA domain of the spastin based on template crystal structures of VPS4B monomer and p97/VCP hexamer. The structural model of spastin provided us with a framework to determine

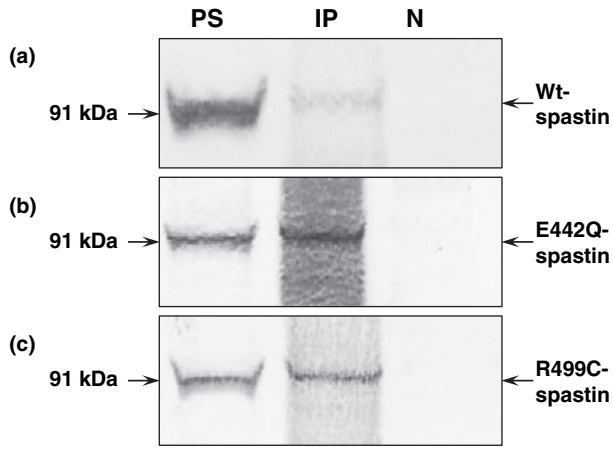

Fig. 4 Immunoprecipitation assay. To determine the interaction between spastin monomers, *ex vivo* immunoprecipitation assay was performed. The soluble total protein extract from NIH3T3 cells co-transfected with c-Myc-spastin and Gfp-spastin constructs was immunoprecipitated with c-Myc antibody and subsequently western blot was performed with Gfp antibody. Lane 1 (PS), corresponds to standard protein lysate, which serves as a control for transfection efficiency; lane 2 (IP), immunoprecipitated fraction; lane 3 (N), mock precipitation was performed without c-Myc antibody. A band sized 91 kDa corresponding to Gfp-spastin can be seen in lane PS and lane IP but not in lane N (a). Similarly, when immunoprecipitation was carried out between wild-type c-Myc-spastin and mutated Gfp-spastin (E442Q-spastin), c-Myc-spastin was able to immunoprecipitate E442Q-spastin (b). Also interaction between c-Myc-spastin and R499C-spastin could be confirmed by immunoprecipitation assay (c).

the residues forming active site, loop structures and monomer-monomer interface residues necessary for oligomerization. Finally, through co-localization studies in mammalian cells, we show E442Q mutant spastin function in dominant negative fashion and causes redistribution of both wild-type spastin monomer and spastin interacting protein RTN1 into MT bundles.

Spastin is a multifaceted protein and exists in several isoforms and probably its different molecular functions are mediated through its various isoforms. The two major isoforms of spastin are the long form starting from M1 codon and an N-terminal truncated (1–86 amino acid) form encoded from M87 named the short isoform (Claudiani *et al.* 2005). The spliced variants lacking exon 4 of either of these isoforms appears to be more relevant for endogenous function as no mutation out of over 220 mutations reported were detected in exon 4. There are conflicting reports concerning physiological relevance of long and short isoform of spastin. A recent study claims that short isoform is predominantly expressed in brain and retains all the physiological function (Salinas *et al.* 2005). Interestingly, it is also reported that the long isoform is enriched in spinal cord when compared with other tissues (Claudiani *et al.* 2005 and Solowska *et al.* 2008); therefore, it is of direct importance for the pathogenesis of HSP. Further studies requiring specific targeting of either of the isoforms of spastin will be necessary to elucidate the isoform specific physiological function of spastin. In the current study, we used the short isoform of spastin for experimental simplicity as this isoform lacks the hydrophobic domain, therefore, it is likely to be more soluble and tendency to form aggregates is minimal. In addition the role of N-terminal region of spastin on the stability of possible oligomeric structure driven by the AAA domain can only be emphasized when the studies are carried out with a full-length form of the protein. The rationale behind using a full-length isoform was further highlighted with the fact that affinity of full-length spastin (long isoform) isoform ($K_m = 0.45 \pm 0.07$ mM) for its substrate ATP is much higher than that of AAA domain of spastin ($K_m = 2.2 \pm 0.63$ mM) (White *et al.* 2007).

The first indication that spastin exists as a higher order oligomeric structure was derived from DSP chemical cross-linking studies. Interestingly, in absence of DSP, a minority of spastin fraction was in oligomeric state and we observed two oligomeric fractions of spastin corresponding to a lower order intermediate form and a higher order, perhaps equivalent to hexameric form. At higher concentration (1.0 mM) of DSP, the predicted hexamer was the predominant form of spastin and both monomeric and intermediate forms were almost negligible suggesting that spastin oligomerization was DSP concentration dependent. To determine the precise number of spastin monomers which constitute the higher order spastin oligomeric structure, we performed gel filtration assay. We demonstrated that approximately six monomers comprise the oligomer thus spastin monomers can assemble into a hexamer. However, in contrast to many AAA proteins, which require ATP/ADP to form oligomers, spastin oligomerization state was independent of nucleotide binding state. Nevertheless, it appears that binding of ATP favors the hexameric conformation, as in gel filtration assay in absence of ATP the oligomeric spastin eluted in a broad spectrum of fractions suggesting spastin exists in numerous oligomeric states. In presence of ATP, spastin hexameric state is stabilized as elution pattern in gel filtration became much narrower and eluted fraction molecular weight corresponded to hexameric spastin. It can be postulated that in absence of ATP, a steady state equilibrium exists between monomer↔intermediate oligomer(s)↔hexamer spastin. However, binding of ATP drives this equilibrium towards hexameric state. The steady state equilibrium model for spastin is also supported by chemical cross-linking study as a minor fraction of intermediate and higher (hexamer) form of spastin could be detected even under non-cross-linking condition. The nucleotide binding induced conformation change from intermediate state to hexamer is also reported for ClpB, a bacterial AAA + ATPase, which is a member of a multichaperone system (Goloubinoff *et al.* 1999; Motohashi *et al.* 1999; Zolkiewski 1999). In the nucleotide free-

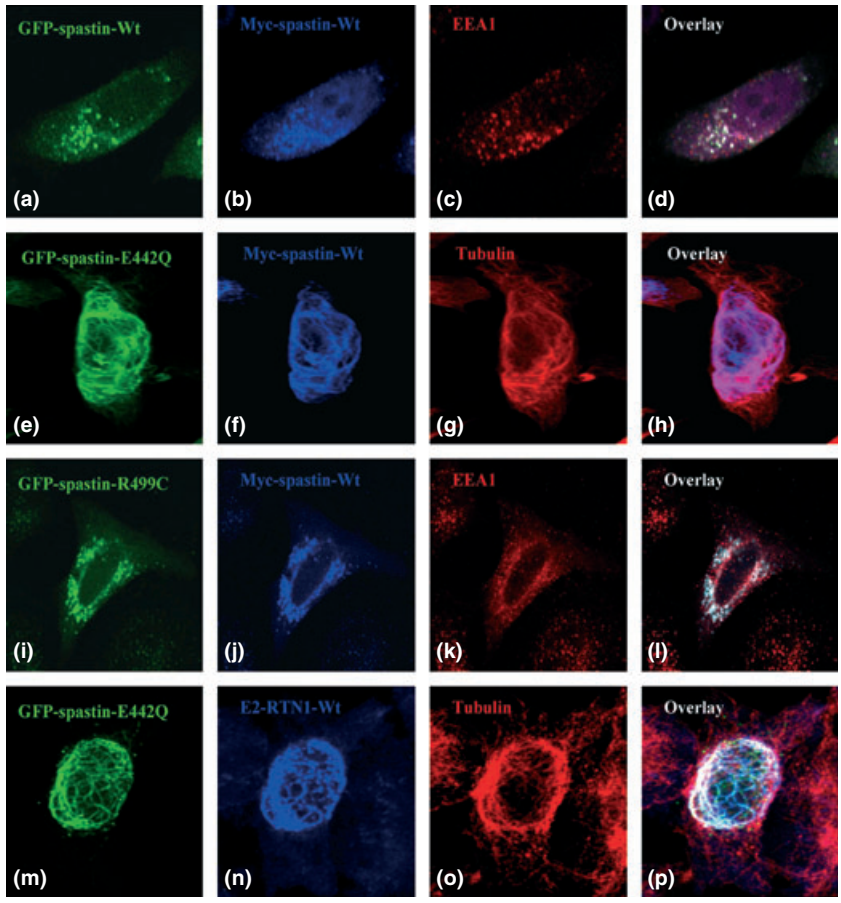

Fig. 5 Co-localization of spastin monomers and RTN1 in mammalian cells. NIH3T3 cells were transiently co-transfected with c-Myc-spastin and Gfp-spastin. Both Gfp-spastin (a) and c-Myc-spastin (b) showed expression in the endosomal vesicle (c) arising from perinuclear region of cell. Overlay of image (a–c) showed strong co-localization of c-Myc-spastin and Gfp-spastin (d). Co-expression of E442Q mutant Gfp-spastin (E442Q-spastin) and wild-type c-Myc-spastin (e–h). E442Q-spastin, showed typical filamentous expression pattern (e), however in the same cell, wild-type c-Myc-spastin expression was redistributed from expected punctate vesicles to filamentous pattern (f). Overlay images (e and f) with microtubule staining (g) revealed complete co-localization of wild-type and mutant spastin (h). Wild-type c-Myc-spastin and mutant R499C-spastin show co-expression in endosomal vesicles (I-L), R499C-spastin (i), c-Myc-spastin (j), EEA1 (k), and overlay (l). Furthermore, co-expression of E442Q mutant spastin and E2-RTN1 (spastin interacting protein) led to misexpression of E2-RTN1 from punctate vesicles to microtubule filament (m–p), E442Q-spastin (m), E2-RTN1 (n), EEA1 (o), and overlay (p).

state, ClpB undergoes reversible self-association that involves protein concentration-dependent population of monomers, heptamers, and intermediate-size oligomers (Akoev *et al.* 2004). In contrast, binding to ATPγS as well as ADP stabilizes the hexameric form of ClpB (Akoev *et al.* 2004). Furthermore, p97/VCP, an AAA family protein, which acts as a molecular chaperone in diverse cellular events, can form hexamers without the addition of nucleotide (Wang *et al.* 2003). The p97/VCP contains an N-terminal substrate-binding domain and two conserved ATPase domains D1 and D2, which are separated from N-terminal domain by a linker motif. This nucleotide-independent hexamerization only requires an intact D1 and the linker sequence of p97/VCP (Wang *et al.* 2003). Besides, it is also reported that spastin MT-associated protein like activity, which promotes MT bundling is also independent of nucleotide binding (Salinas *et al.* 2005). Recently, a study reported that the AAA domain of spastin can assemble into hexamer (White *et al.* 2007). The hexameric state of AAA domain of spastin was very unstable as it could not be stabilized even in the presence of slowly hydrolysable ATPγS and they could only trap the hexamer when they used the Walker B E442Q mutant form of spastin AAA domain. The discrepancy between our observation and this report could be due to the fact that we used entire short isoform of spastin form and they used deleted and modified AAA domain. The full-length spastin is a true representative of endogenous protein and perhaps the N-terminal domain stabilizes the oligomeric state of spastin as also shown for p97/VCP protein in which N-terminal linker motif is necessary for hexamerization (Wang *et al.* 2003). However, our study was not able to conclusively address or exclude the

possibility of the trace amount of bacterial ATP, which might be bound to spastin during purification and gel filtration.

To gain a comprehensive overview of the oligomeric structure of spastin, we generated a model of the AAA domain of spastin using template structures of VPS4B (Scott *et al.* 2005) and p97/VCP (Dreveny *et al.* 2004). The modeled tertiary structure of spastin preserves the overall structural architecture of a typical AAA domain, which is defined by two central domains: an amino-proximal α/β domain and a smaller four-helix bundle. Additionally, the modeled spastin also consists of an N-terminal β sheet (β′) and a C-terminal α helix, which is also reported in VPS4B (Babst *et al.* 1998; Scott *et al.* 2005). These structural variants appear to be characteristics of the meiotic clade of AAA ATPases, which also include fidgetin and katanin (p60) (Frickey and Lupas 2004) and in this respect, the meiotic subgroups appears distinct from other AAA proteins. However, several structural features are different among structures used as templates and spastin model. For example, comparative analysis indicates that the region of monomeric VPS4B (Scott *et al.* 2005), aligning with α′ helical region of the hexameric p97/VCP crystal structure (Dreveny *et al.* 2004), adopts a different conformation. Comparison of the monomeric and hexameric crystal structures of the homologs suggests that regions α′ and α1 helix undergo conformational change between monomeric and hexameric forms. For these reasons, the α′ and α1 regions in the tertiary structural model of spastin were generated using the equivalent regions of p97/VCP crystal structure. Furthermore the loop structures of spastin model are variable compared with the templates.

Most AAA ATPases function as oligomeric rings, usually a hexamer and previously, p97/VCP was crystallized as a hexamer with bound ADP (Dreveny *et al.* 2004). The similarity between spastin and p97/VCP allowed us to model oligomeric state of spastin by simply overlaying six spastin subunits onto hexameric p97/VCP, which produced a feasible model with no major steric clashes. In fact, most residues that make up the protein-protein interfaces between monomers are conserved between p97/VCP and spastin, indicating that the two hexameric assemblies are likely to be conserved. Taken together, our gel filtration and modeling data, it favors the idea that spastin oligomerizes into hexameric ring. The C-terminal end helix of spastin, which appears to be the property of meiotic clade, in VPS4B forms an exposed annulus on one side of the hexameric ring, which is suggested to mediate ring dimerization and thereby stabilize a double-ring structure (Scott *et al.* 2005). Therefore, higher order hexamer possibly a dodecamer structure for spastin cannot be completely ruled out.

The model of spastin provides us with a framework to classify the identified missense mutations in the AAA domain from HSP patients into structural/functional groups. We categorized the known missense mutations reported in database as active site, monomer-monomer interaction, pore-loop and unknown structural group of mutations. The present classification of missense mutations in AAA domain will facilitate our understanding of molecular function of different subdomains of spastin. In future, it will enable us to classify an identified sequence variant in a HSP patient as disease causing mutation with greater level of confidence. In addition, more information concerning the functional implication of identified mutation can be deciphered from the spastin model.

However, recently (while our paper was in revision), a crystal structure of *Drosophila* spastin AAA domain was reported (Roll-Mecak and Vale 2008), which also suggest that spastin forms a hexamer ring with a prominent central pore and six radiating arms that may dock onto the MT. Their study revealed that the spastin apoenzyme exists in equilibrium between monomeric↔ dimeric (intermediate) forms, whereas binding of ATP favors the hexameric conformation, which was comparable to our findings. Furthermore, findings from Roll-Mecak and Vale regarding the role of N-terminal region (the linker and MIT domain) acting as stabilizing factor for the hexameric structure is supportive of our data, which also point out that N-terminal region is required for a stable formation of hexamer.

Next, we went on to validate that spastin indeed functions as oligomer in the mammalian cells by *ex vivo* immunoprecipitation and co-localization studies. Remarkably, when we used ATPase-defective E442Q mutant of spastin, which binds to ATP, however is unable to hydrolyze it (Evans *et al.* 2005), in *ex vivo* co-localization study, we observed redistribution of wild-type spastin from punctate vesicles to filamentous pattern, where it co-localized with E442Q. Also, co-expression of the E442Q mutant spastin with RTN1, a previously characterized spastin interacting protein (Mannan *et al.* 2006a) caused misexpression of RTN1 to filament instead of typical punctate vesicular expression. Previously, a similar redistribution effect of mutant spastin was also reported between wild-type/K338R-spastin (Errico *et al.* 2002), atlastin/E442Q-spastin (Evans *et al.* 2005) and atlastin/K338R-spastin (Sanderson *et al.* 2006). Furthermore, several known disease causing mutations shows filamentous pattern of expression, such as I344K, N386K, K388R, and R424G (Ki *et al.* 2002; Errico *et al.* 2002; McDermott *et al.* 2003; Evans *et al.* 2005). These mutations most likely depict the substrate entrapped state of the enzyme and most likely will render a dominant negative function by causing redistribution of wild-type spastin.

Mutational screen have identified over 224 different mutations in spastin, which include all types of mutations such as missense, nonsense, splice site mutations, and insertions/deletions. This wide spectrum of mutation led to a generalized perception that underlying cause for spastin-associated HSP is haploinsufficiency and degeneration of axons results from failure to achieve a threshold level of spastin for normal MT severing. However, presence

of another MT-severing protein, P60-katanin, which shows an overlapping expression pattern with spastin and is expressed at much higher level compared with spastin (Yu *et al.* 2005 and Solowska *et al.* 2008) further demur the 'loss of function model' for spastin. Moreover, a knockout mouse lacking functional spastin showed only late and mild form of degeneration and no detectable abnormalities during development (Tarrade *et al.* 2006). Contrarily, in a recent study, Solowska *et al.* (2008) showed that over-expression of a truncated form of long isoform of spastin depicts deleterious effects to axonal growth and inhibits fast axonal transport, which is consistent with a 'gain of function' mechanism.

However, to resolve the issue of 'gain/loss of function' further *in vivo* model systems including knockin and transgenic mouse models should be devised for various types of spastin disease causing mutations. These different pathomechanism models for mutant spastin mode of action need to be carefully resolved by experimental means; otherwise there will be repercussion on the likely success on any therapeutical approach devised for spastin-associated HSP.

Acknowledgements

The authors would like to thank H. Hühn and K. Neifer for excellent technical assistance and M. Mariappan and U. Winter for helping us with gel filtration chromotagraphy. We would also like to thank E. I. Rugarli for kindly providing us with spastin polyclonal antibody. NS thanks Department of Biotechnology (India), for the support. LSS is supported by a fellowship from Council of Scientific and Industrial Research (India). This work was funded partly by the Deutsche Forschungsgemeinschaft Grant (Germany) and Tom Wahlig Stiftung Grant (Germany) to AUM.

Supplementary material

The following supplementary material is available for this article:

Table S1. Interaction environment on one oligomerisation surface.

Table S2. Interaction environment on another oligomerisation surface.

Table S3. Classification of known set of disease associated HSP missense mutations in AAA domain into different structural category.

Fig. S1. Purification and enzymatic ATPase assay of recombinant spastin.

Fig. S2. Alignment used for modeling AAA ATPase domain of spastin.

This material is available as part of the online article from: http://www.blackwell-synergy.com/doi/abs/10.1111/j.1471-4159.2008.05414.x (This link will take you to the article abstract).

Please note: Blackwell Publishing is not responsible for the content or functionality of any supplementary materials supplied by the authors. Any queries (other than missing material) should be directed to the corresponding author for the article.

Statement of competing interests

The authors declare that they have no competing interests.

References

Akoev V., Gogol E. P., Barnett M. E. and Zolkiewski M. (2004) Nucleotide-induced switch in oligomerization of the AAA+ ATPase ClpB. *Protein Sci.* **13**, 567–574.

Altschul S. F., Madden T. L., Schaffer A. A., Zhang J., Zhang Z., Miller W. and Lipman D. J. (1997) Gapped BLAST and PSI-BLAST: a new generation of protein database search programs. *Nucleic Acids Res.* **25**, 3389–3402.

Babst M., Wendland B., Estepa E. J. and Emr S. D. (1998) The Vps4p AAA ATPase regulates membrane association of a Vps protein complex required for normal endosome function. *EMBO J.* **17**, 2982–2993.

Berman H. M., Westbrook J., Feng Z., Gilliland G., Bhat T. N., Weissig H., Shindyalov I. N. and Bourne P. E. (2000) The protein data bank. *Nucleic Acids Res.* **28**, 235–242.

Ciccarelli F. D., Proukakis C., Patel H., Cross H., Azam S., Patton M. A., Bork P. and Crosby A. H. (2003) The identification of a conserved domain in both spartin and spastin, mutated in hereditary spastic paraplegia. *Genomics* **81**, 437–441.

Claudiani P., Riano E., Errico A., Andolfi G. and Rugarli E. I. (2005) Spastin subcellular localization is regulated through usage of different translation start sites and active export from the nucleus. *Exp. Cell Res.* **309**, 358–369.

Confalonieri F. and Duguet M. (1995) A 200-amino acid ATPase module in search of a basic function. *Bioessays* **17**, 639–650.

Dreveny I., Kondo H., Uchiyama K., Shaw A., Zhang X. and Freemont P. S. (2004) Structural basis of the interaction between the AAA ATPase p97/VCP and its adaptor protein p47. *EMBO J.* **23**, 1030–1039.

Errico A., Ballabio A. and Rugarli E. I. (2002) Spastin, the protein mutated in autosomal dominant hereditary spastic paraplegia, is involved in microtubule dynamics. *Hum. Mol. Genet.* **11**, 153–163.

Errico A., Claudiani P., D'Addio M. and Rugarli E. I. (2004) Spastin interacts with the centrosomal protein NA14, and is enriched in the spindle pole, the midbody and the distal axon. *Hum. Mol. Genet.* **13**, 2121–2132.

Evans K. J., Gomes E. R., Reisenweber S. M., Gundersen G. G. and Lauring B. P. (2005) Linking axonal degeneration to microtubule remodeling by spastin-mediated microtubule severing. *J. Cell Biol.* **168**, 599–606.

Evans K., Keller C., Pavur K., Glasgow K., Conn B. and Lauring B. (2006) Interaction of two hereditary spastic paraplegia gene products, spastin and atlastin, suggests a common pathway for axonal maintenance. *Proc. Natl Acad. Sci. USA* **103**, 10666–10671.

Fink J. K. (2003) The hereditary spastic paraplegias: nine genes and counting. *Arch. Neurol.* **60**, 1045–1049.

Fonknechten N., Mavel D., Byrne P. *et al.* (2000) Spectrum of SPG4 mutations in autosomal dominant spastic paraplegia. *Hum. Mol. Genet.* **9**, 637–644.

Frickey T. and Lupas A. N. (2004) Phylogenetic analysis of AAA proteins. *J. Struct. Biol.* **146**, 2–10.

Goloubinoff P., Mogk A., Zvi A. P., Tomoyasu T. and Bukau B. (1999) Sequential mechanism of solubilization and refolding of stable protein aggregates by a bichaperone network. *Proc. Natl Acad. Sci. USA* **96**, 13732–13737.

Hanson P. I. and Whiteheart S. W. (2005) AAA+ proteins: have engine, will work. *Nat. Rev. Mol. Cell Biol.* **6**, 519–529.

Harding A. E. (1983) Classification of the hereditary ataxias and paraplegias. *Lancet* **1**, 1151–1155.

Hartman J. J. and Vale R. D. (1999) Microtubule disassembly by ATP-dependent oligomerization of the AAA enzyme katanin. *Science* **286**, 782–785.

Hazan J., Fonknechten N., Mavel D. *et al.* (1999) Spastin, a new AAA protein, is altered in the most frequent form of autosomal dominant spastic paraplegia. *Nat. Genet.* **23**, 296–303.

Ki C. S., Lee W. Y., Han D. H. *et al.* (2002) A novel missense mutation (I344K) in the SPG4gene in a Korean family with autosomal-dominant hereditary spastic paraplegia. *J. Hum. Genet.* **47**, 473–477.

Lindsey J. C., Lusher M. E., McDermott C. J., White K. D., Reid E., Rubinsztein D. C., Bashir R., Hazan J., Shaw P. J. and Bushby K. M. (2000) Mutation analysis of the spastin gene (SPG4) in patients with hereditary spastic paraparesis. *J. Med. Genet.* **37**, 759–765.

Luthy R., Bowie J. U. and Eisenberg D. (1992) Assessment of protein models with three-dimensional profiles. *Nature* **356**, 83–85.

Mannan A. U., Boehm J., Sauter S. M., Rauber A., Byrne P. C., Neesen J. and Engel W. (2006a) Spastin, the most commonly mutated protein in hereditary spastic paraplegia interacts with reticulon 1 an endoplasmic reticulum protein. *Neurogenetics* **7**, 93–103.

Mannan A. U., Krawen P., Sauter S. M., Boehm J., Chronowska A., Paulus W., Neesen J. and Engel W. (2006b) ZFYVE27 (SPG33), a novel spastin-binding protein, is mutated in hereditary spastic paraplegia. *Am. J. Hum. Genet.* **79**, 351–357.

McDermott C. J., Grierson A. J., Wood J. D., Bingley M., Wharton S. B., Bushby K. M. and Shaw P. J. (2003) Hereditary spastic paraparesis: disrupted intracellular transport associated with spastin mutation. *Ann. Neurol.* **54**, 748–759.

McNally F. J. and Vale R. D. (1993) Identification of katanin, an ATPase that severs and disassembles stable microtubules. *Cell* **75**, 419–429.

Motohashi K., Watanabe Y., Yohda M. and Yoshida M. (1999) Heat-inactivated proteins are rescued by the DnaK.J-GrpE set and ClpB chaperones. *Proc. Natl Acad. Sci. USA* **96**, 7184–7189.

Patel S. and Latterich M. (1998) The AAA team: related ATPases with diverse functions. *Trends Cell Biol.* **8**, 65–71.

Patel H., Cross H., Proukakis C., Hershberger R., Bork P., Ciccarelli F. D., Patton M. A., McKusick V. A. and Crosby A. H. (2002) SPG20 is mutated in Troyer syndrome, an hereditary spastic paraplegia. *Nat. Genet.* **31**, 347–348.

Reid E., Connell J., Edwards T. L., Duley S., Brown S. E. and Sanderson C. M. (2005) The hereditary spastic paraplegia protein spastin interacts with the ESCRT-III complex-associated endosomal protein CHMP1B. *Hum. Mol. Genet.* **14**, 19–38.

Roll-Mecak A. and Vale R. D. (2005) The *Drosophila* homologue of the hereditary spastic paraplegia protein, spastin, severs and disassembles microtubules. *Curr. Biol.* **15**, 650–655.

Roll-Mecak A. and Vale R. D. (2008) Structural basis of microtubule severing by the hereditary spastic paraplegia protein spastin. *Nature* **451**, 363–367.

Sali A. (1995) Comparative protein modeling by satisfaction of spatial restraints. *Mol. Med. Today* **1**, 270–277.

Salinas S., Carazo-Salas R. E., Proukakis C., Cooper J. M., Weston A. E., Schiavo G. and Warner T. T. (2005) Human spastin has multiple microtubule-related functions. *J. Neurochem.* **95**, 1411–1420.

Sanderson C. M., Connell J. W., Edwards T. L., Bright N. A., Duley S., Thompson A., Luzio J. P. and Reid E. (2006) Spastin and atlastin, two proteins mutated in autosomal-dominant hereditary spastic paraplegia, are binding partners. *Hum. Mol. Genet.* **15**, 307–318.

Scott A., Chung H. Y., Gonciarz-Swiatek M. *et al.* (2005) Structural and mechanistic studies of VPS4 proteins. *EMBO J.* **24**, 3658–3669.

Sherwood N. T., Sun Q., Xue M., Zhang B. and Zinn K. (2004) *Drosophila* spastin regulates synaptic microtubule networks and is required for normal motor function. *PLoS Biol.* **2**, e429.

Sobolev V., Sorokine A., Prilusky J., Abola E. E. and Edelman M. (1999) Automated analysis of interatomic contacts in proteins. *Bioinformatics* **15**, 327–332.

Solowska J. M., Morfini G., Falnikar A., Himes B. T., Brady S. T., Huang D. and Baas P. W. (2008) Quantitative and functional analyses of spastin in the nervous system: implications for hereditary spastic paraplegia. *J. Neurosci.* **28**, 2147–2157.

Tarrade A., Fassier C., Courageot S. *et al.* (2006) A mutation of spastin is responsible for swellings and impairment of transport in a region of axon characterized by changes in microtubule composition. *Hum. Mol. Genet.* **15**, 3544–3558.

Trotta N., Orso G., Rossetto M. G., Daga A. and Broadie K. (2004) The hereditary spastic paraplegia gene, spastin, regulates microtubule stability to modulate synaptic structure and function. *Curr. Biol.* **14**, 1135–1147.

Wang Q., Song C., Yang X. and Li C. C. (2003) D1 ring is stable and nucleotide-independent, whereas D2 ring undergoes major conformational changes during the ATPase cycle of p97-VCP. *J. Biol. Chem.* **278**, 32784–32793.

White S. R., Evans K. J., Lary J., Cole J. L. and Lauring B. (2007) Recognition of C-terminal amino acids in tubulin by pore loops in spastin is important for microtubule severing. *J. Cell Biol.* **176**, 995–1005.

Wood J. D., Landers J. A., Bingley M., McDermott C. J., Thomas-McArthur V., Gleadall L. J., Shaw P. J. and Cunliffe V. T. (2006) The microtubule-severing protein spastin is essential for axon outgrowth in the zebrafish embryo. *Hum. Mol. Genet.* **15**, 2763–2771.

Yoshimori T., Yamagata F., Yamamoto A., Mizushima N., Kabeya Y., Nara A., Miwako I., Ohashi M., Ohsumi M. and Ohsumi Y. (2000) The mouse SKD1, a homologue of yeast Vps4p, is required for normal endosomal trafficking and morphology in mammalian cells. *Mol. Biol. Cell* **11**, 747–763.

Yu W., Solowska J. M., Qiang L., Karabay A., Baird D. and Baas P. W. (2005) Regulation of microtubule severing by katanin subunits during neuronal development. *J. Neurosci.* **25**, 5573–5583.

Zolkiewski M. (1999) ClpB cooperates with DnaK, DnaJ, and GrpE in suppressing protein aggregation. A novel multi-chaperone system from *Escherichia coli*. *J. Biol. Chem.* **274**, 28083–28086.